
This is an electronic reprint of the original article.
This reprint *may differ* from the original in pagination and typographic detail.

Author(s): Carroll, R. J.; Page, R. D.; Joss, D. T.; O'Donnell, D.; Uusitalo, Juha; Darby, I. G.; Andgren, K.; Auranen, Kalle; Bönig, S.; Cederwall, B.; Doncel, M.; Drummond, M. C.; Eeckhautd, Sarah; Grahn, Tuomas; Gray-Jones, C.; Greenlees, Paul; Hadinia, B.; Herzan, Andrej; Jakobsson, Ulrika; Jones, Peter; Julin, Rauno; Juutinen, Sakari; Konki, Joonas; Kröll, T.; Leino, Matti; Leppänen, Ari-Pekka; McPeake, C.; Nyman, Markus; Pakarinen, Janna; Pastore, Jari; Paves, Pauli; Pekkila, Panu; Revill, L.; Ruotsalainen, Jari
Title: Excited states in the proton-unbound nuclide ^{158}Ta

Year: 2016

Version:

Please cite the original version:

Carroll, R. J., Page, R. D., Joss, D. T., O'Donnell, D., Uusitalo, J., Darby, I. G., Andgren, K., Auranen, K., Bönig, S., Cederwall, B., Doncel, M., Drummond, M. C., Eeckhautd, S., Grahn, T., Gray-Jones, C., Greenlees, P., Hadinia, B., Herzan, A., Jakobsson, U., . . . Thornthwaite, A. (2016). Excited states in the proton-unbound nuclide ^{158}Ta . *Physical Review C*, 93(3), Article 034307.
<https://doi.org/10.1103/PhysRevC.93.034307>

All material supplied via JYX is protected by copyright and other intellectual property rights, and duplication or sale of all or part of any of the repository collections is not permitted, except that material may be duplicated by you for your research use or educational purposes in electronic or print form. You must obtain permission for any other use. Electronic or print copies may not be offered, whether for sale or otherwise to anyone who is not an authorised user.

Excited states in the proton-unbound nuclide ^{158}Ta

R. J. Carroll,^{1,*} R. D. Page,¹ D. T. Joss,¹ D. O'Donnell,^{1,†} J. Uusitalo,² I. G. Darby,^{1,‡} K. Andgren,³ K. Auranen,² S. Bönig,⁴ B. Cederwall,³ M. Doncel,³ M. C. Drummond,¹ S. Eeckhaudt,² T. Grahn,² C. Gray-Jones,¹ P. T. Greenlees,² B. Hadinia,^{3,§} A. Herzán,² U. Jakobsson,^{2,¶} P. M. Jones,^{2,**} R. Julin,² S. Juutinen,² J. Konki,² T. Kröll,⁴ M. Leino,² A.-P. Leppänen,^{2,††} C. McPeake,¹ M. Nyman,^{2,‡‡} J. Pakarinen,² J. Partanen,² P. Peura,^{2,§§} P. Rahkila,² J. Revill,¹ P. Ruotsalainen,^{2,¶¶} M. Sandzelius,^{2,3} J. Sarén,² B. Saygi,¹ C. Scholey,² D. Seweryniak,⁵ J. Simpson,⁶ J. Sorri,² S. Stolze,² M. J. Taylor,⁷ and A. Thornthwaite¹

¹*Oliver Lodge Laboratory, University of Liverpool, Liverpool L69 7ZE, United Kingdom*

²*University of Jyväskylä, Department of Physics, FI-40014 Jyväskylä, Finland*

³*Royal Institute of Technology, Department of Physics, Alba Nova Centre, S-106 91 Stockholm, Sweden*

⁴*Institut für Kernphysik, Technische Universität Darmstadt, D-64289 Darmstadt, Germany*

⁵*Argonne National Laboratory, Argonne, Illinois 60439, USA*

⁶*STFC Daresbury Laboratory, Daresbury, Warrington WA4 4AD, United Kingdom*

⁷*Schuster Laboratory, University of Manchester, Manchester M13 9PL, United Kingdom*

(Received 2 December 2015; revised manuscript received 22 January 2016; published 8 March 2016)

Excited states in the neutron-deficient odd-odd proton-unbound nuclide ^{158}Ta have been investigated in two separate experiments. In the first experiment, ^{166}Ir nuclei were produced in the reactions of 380 MeV ^{78}Kr ions with an isotopically enriched ^{92}Mo target. The α -decay chain of the 9^+ state in ^{166}Ir was analyzed. Fine structure in the α decay of the 9^+ state in ^{162}Re established a 66 keV difference in excitation energy between the lowest-lying 9^+ and 10^+ states in ^{158}Ta . Higher-lying states in ^{158}Ta were populated in the reactions of 255 MeV ^{58}Ni ions with an isotopically enriched ^{102}Pd target. Gamma-ray decay paths that populate, depopulate, and bypass a 19^- isomeric state have been identified. The general features of the deduced level scheme are discussed and the prospects for observing proton emission branches from excited states are considered.

DOI: [10.1103/PhysRevC.93.034307](https://doi.org/10.1103/PhysRevC.93.034307)

I. INTRODUCTION

Nuclei at the boundaries of the nuclear landscape are an important testing ground for models of nuclear properties. Current experimental techniques offer possibilities to investigate excited states in nuclei beyond the proton drip line, probing discrete states that are highly unbound to proton emission. Despite the low production cross sections for such neutron-deficient nuclei, extensive level schemes have been

produced for proton-unbound nuclides, including many proton emitters [1–13]. In some cases the level schemes extend to excitation energies of several MeV.

In the majority of nuclei studied to date, it appears that the retarding effect of the potential barrier through which the protons have to tunnel in order to be emitted allows γ -ray emission to dominate. In heavy odd-odd nuclei near closed shells certain configurations can be energetically favored, resulting in states for which γ -decay lifetimes are comparatively long. If such isomers are proton-unbound, they are potentially of interest as candidates for proton-emitting states. One challenge with odd-odd nuclei is that their excitation level schemes are very complicated. Proton-decay half-lives can increase by an order of magnitude if the decay Q value decreases by of order 100 keV or the orbital angular momentum of the emitted proton increases by $1 \hbar$ [14]. This makes obtaining sufficiently precise theoretical predictions that would allow potential proton-emitting states to be chosen for experimental study extremely challenging. However, if excited states are established experimentally in nuclei beyond the proton drip line, this information can be used in calculating proton-decay branches, either to guide experimental searches or to compare with measurements.

The nuclide ^{158}Ta is the lightest $N = 85$ isotone to be located beyond the proton drip line [15]. Prior to the discovery of the 19^- isomeric state and its decay by α -particle emission and γ -ray emission [16,17], only two states were known in ^{158}Ta , both of which decay by α -particle emission: the (2^-) ground state and a 9^+ state lying at an excitation energy of 141(9) keV [18]. In this paper we present further details of the γ -decay paths from the 19^- isomer, together with information on the

*Present address: Department of Physics, University of Surrey, Guildford GU2 7XH, United Kingdom.

†Present address: Department of Physics, University of Glasgow, Glasgow G12 8QQ, United Kingdom.

‡Present address: Department of Nuclear Sciences and Applications, International Atomic Energy Agency, A-1400 Vienna, Austria.

§Present address: Department of Physics, University of Guelph, Guelph, Ontario, N1G 2W1 Canada.

¶Present address: Royal Institute of Technology, Department of Physics, Alba Nova Centre, S-106 91 Stockholm, Sweden.

**Present address: Department of Nuclear Physics, iThemba Laboratory for Accelerator Based Sciences, PO Box 722, Somerset West 7129, South Africa.

††Present address: STUK, Radiation and Nuclear Safety Authority, Finland.

‡‡Present address: Institute for Reference Materials and Measurements (IRMM), Retieseweg 111, B-2440 Geel, Belgium.

§§Present address: Helsinki Institute of Physics, FI-00014, University of Helsinki, Finland.

¶¶Present address: TRIUMF, 4004 Wesbrook Mall, Vancouver, British Columbia V6T 2A3, Canada.

γ -ray transitions that populate it and others that form decay paths that bypass it, feeding instead the 9^+ - α -decaying state.

II. EXPERIMENTAL DETAILS

The data were obtained from two separate experiments performed at the Accelerator Laboratory at the University of Jyväskylä. The first experiment investigated the α -decay chain of the 9^+ state in ^{166}Ir through the corresponding state in ^{162}Re to states in ^{158}Ta [18]. The ^{166}Ir nuclei were produced by irradiating a ^{92}Mo target of $\sim 0.6 \text{ mg cm}^{-2}$ thickness and 94% isotopic enrichment with a beam of 380 MeV ^{78}Kr ions. The beam was delivered for approximately 276 h with an average beam intensity of 2.9 particle nA. The nuclei produced in the fusion evaporation reactions recoiled out of the target into the gas-filled separator RITU [19] and were transported to the GREAT spectrometer [20]. The nuclei passed through a multiwire proportional counter (MWPC) and were implanted into a pair of double-sided silicon strip detectors (DSSDs). Discrimination between evaporation residues and scattered beam particles was achieved on the basis of the energy loss of ions in the MWPC and their flight time between the MWPC and the DSSDs. Decay particles in the DSSDs were distinguished by demanding anticoincidences with the MWPC. Each of the DSSDs had an active area of $60 \text{ mm} \times 40 \text{ mm}$, a thickness of $300 \mu\text{m}$, and a strip pitch of 1 mm on both faces, giving a total of 4800 independent pixels. A planar double-sided germanium strip detector was mounted a few mm behind the DSSDs inside the same vacuum enclosure to measure x rays and low-energy γ rays. It had an active area of $120 \text{ mm} \times 60 \text{ mm}$, a thickness of 15 mm, and a strip pitch of 5 mm. A clover Ge detector was mounted above the DSSDs, outside the vacuum chamber and was used to measure higher-energy γ rays.

The second experiment investigated excited states in ^{158}Ta using the same experimental systems, with the addition of the JUROGAM spectrometer to measure the energies of γ rays emitted at the target position. During this experiment JUROGAM consisted of 43 Compton-suppressed Ge detectors. Excited states in ^{158}Ta were populated in fusion

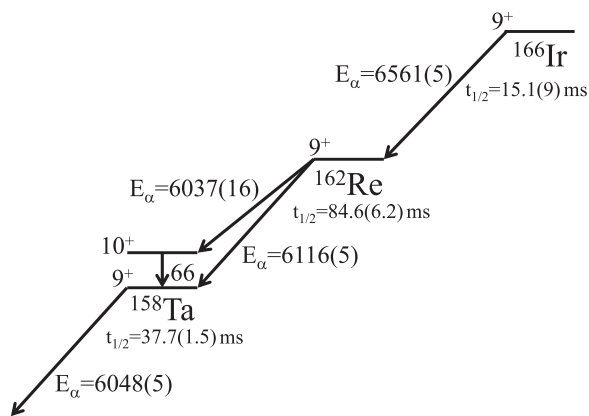


FIG. 1. Schematic α -decay chain from the 9^+ state in ^{166}Ir to states in ^{158}Ta . Fine structure in the α decay of ^{162}Re populating the 10^+ state in ^{158}Ta was identified in the present work. The α -particle energies for the remaining decays and the half-lives in ms are taken from ref. [18]. The α -particle and γ -ray energies are given in keV.

evaporation reactions induced by a beam of 255 MeV ^{58}Ni ions bombarding a ^{102}Pd target foil having a thickness of $\sim 1 \text{ mg cm}^{-2}$ and 90% isotopic enrichment. The beam was delivered at an average intensity of 4.3 particle nA for approximately 139 h. Recoiling nuclei were identified using the recoil-decay tagging technique [21,22] and were correlated in time with their associated γ -ray emissions.

All detector signals from both experiments were passed to the triggerless total data readout data acquisition system [23], where they were time stamped with a precision of 10 ns. The data were analysed using the GRAIN [24] and RADWARE [25] software packages.

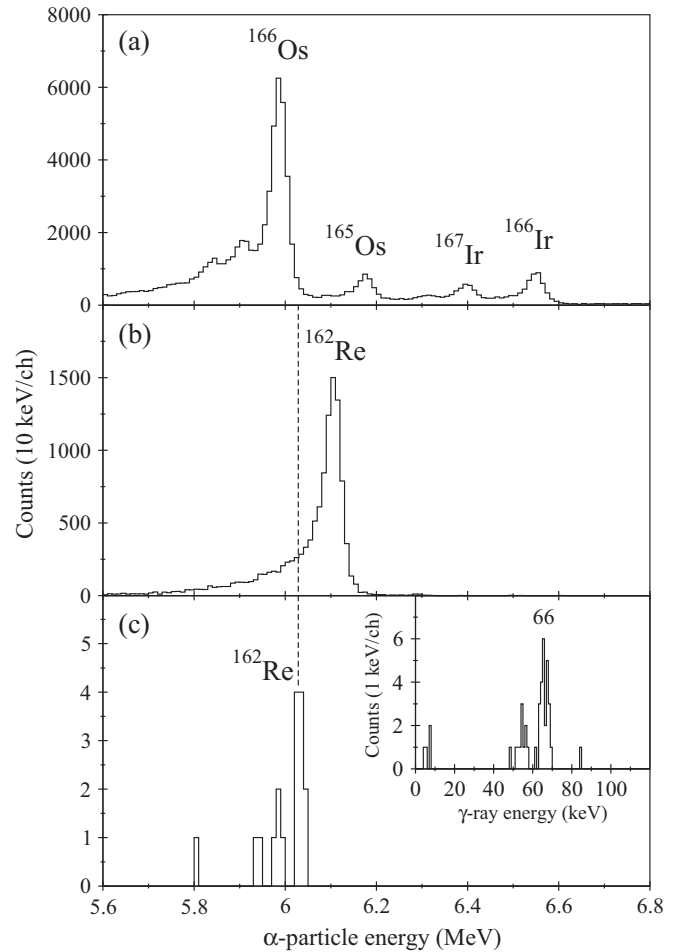


FIG. 2. (a) Energy spectrum of α decays occurring within 50 ms of an ion being implanted into the same DSSD pixel during the first experiment. Assignments for some of the principal peaks are indicated. (b) Energy spectrum of α decays occurring within 250 ms of a ^{166}Ir α decay from (a) in the same DSSD pixel. The ^{166}Ir α decays were required to be in the energy range $E_\alpha = 6490\text{--}6600 \text{ keV}$. (c) The inset shows the energy spectrum of γ rays measured in the planar Ge detector in coincidence with the ^{162}Re α decays in (b) with $E_\alpha \leq 6200 \text{ keV}$, while the main section shows the energy spectrum of α decays from (b) that are in coincidence with the 66 keV γ rays. This 6037(16) keV activity is assigned as fine structure in the α decay of ^{162}Re .

III. RESULTS

Previous studies of ^{166}Ir [18,26,27] have established that the α decay of its low-lying isomer populates the corresponding state in ^{162}Re , which in turn α decays to ^{158}Ta (see Fig. 1). Davids *et al.* proposed spin-parity assignments of 9^+ for these states and 2^- for the corresponding ground states [18]. In the first experiment of the present work, fine structure has been identified in the α decay of the 9^+ isomer in ^{162}Re , establishing the excitation energy of the first excited state above the 9^+ α -decaying isomer in ^{158}Ta .

Figure 2(a) shows the energy spectrum of α decays occurring within 50 ms of the implantation of an ion into the same DSSD pixel. The known α -decay peak of ^{166}Ir is

clearly visible in this spectrum. The energy spectrum of α decays that follow these ^{166}Ir decays within 250 ms is shown in Fig. 2(b). The spectrum is dominated by the known α -decay peak of ^{162}Re . In order to identify fine structure in this peak, γ rays occurring in prompt coincidence with the α decays from Fig. 2(b) were sought. The inset to Fig. 2(c) shows the coincidence energy spectrum observed in the planar Ge detector, revealing a peak at 66 keV. Confirmation that these γ rays are associated with fine structure in the α decay of ^{162}Re can be seen in Fig. 2(c), which shows the energies of α particles observed in coincidence with γ rays in the 66 keV peak. The energy of this α -decay peak is 6037(16) keV. When the corresponding Q value is combined with the γ -ray energy, the

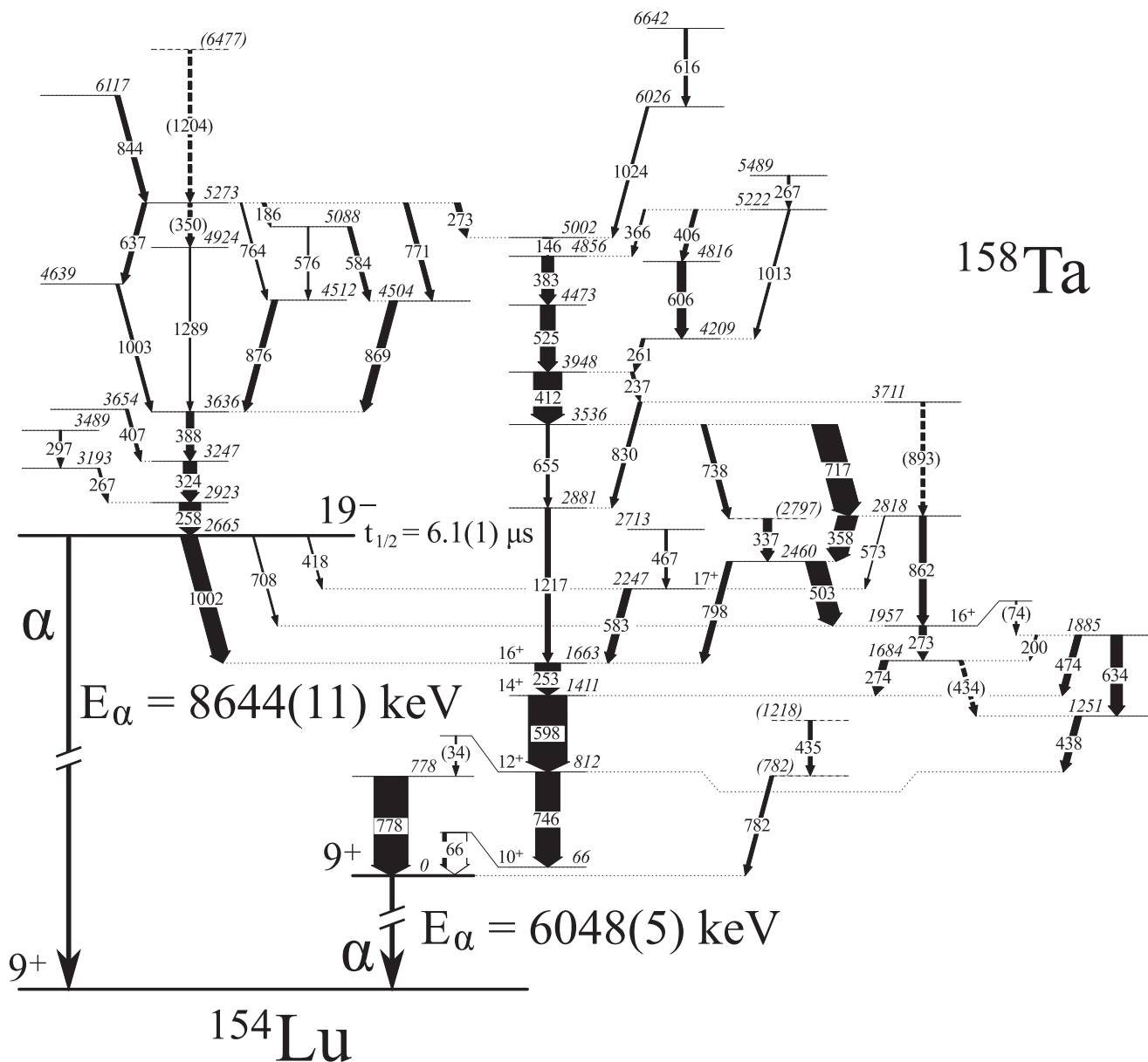


FIG. 3. Proposed level scheme of ^{158}Ta . The widths of the arrows are proportional to the measured intensities in JUROGAM, except for transitions seen only at the focal plane, for which the arrow widths are proportional to intensities measured in the clover detector. Tentative transitions are indicated with dashed arrows with energies in parentheses, while tentative levels are indicated by dashed lines and level energies in parentheses. The α -decay energy of the 9^+ state is taken from Ref. [18]. The spin and parity assignments have been adopted from Ref. [16].

TABLE I. Energies and relative intensities of γ -ray transitions observed at the target position using the JUROGAM spectrometer in the present work. Transitions marked with an asterisk (*) are unresolved doublets or triplets. In some cases, γ - γ coincidences have been used to isolate the individual constituents of a multiplet, distinguishing their centroids and allowing their relative intensities to be deduced. However, the relative intensities of the 358 keV and 359 keV transitions could not be determined, so their combined intensity is given for the 358 keV transition.

E_γ (keV)	I_γ (Prompt)	E_γ (keV)	I_γ (Prompt)	E_γ (keV)	I_γ (Prompt)	E_γ (keV)	I_γ (Prompt)
146.0(1)	141(3)	382.8(1)	290(6)	606.3(1)	223(6)	844.0(2)	135(7)
185.9(1)	60(3)	388.5(1)	180(5)	615.7(2)	88(5)	861.4(2)	187(6)
200.2(2)	36(2)	406.1(1)*	98(11)	633.7(2)	359(28)	868.9(2)	198(5)
236.9(1)	85(3)	406.6(1)*	76(10)	636.7(7)	57(27)	876.3(2)	141(5)
252.9(1)	589(5)	412.1(1)	714(6)	655.2(2)	64(5)	1003.1(2)	93(5)
257.7(1)	497(5)	435.3(1)	472(7)	685.8(2)	104(5)	1013.4(3)	70(5)
261.0(1)	66(3)	438.5(1)	173(5)	716.5(1)	640(7)	1023.8(2)	79(5)
266.8(1)	55(3)	466.6(2)	61(4)	727.5(2)	94(5)	1052.5(3)	50(4)
269.8(2)	49(3)	474.0(1)	143(4)	737.7(2)	130(5)	1074.1(3)	42(4)
273.1(1)*	294(4)	503.3(1)	476(6)	746.3(1)	620(7)	1203.9(2)	147(10)
285.7(2)	26(4)	525.2(1)	397(7)	763.5(2)	56(4)	1217.5(2)	132(10)
296.6(1)	49(3)	537.2(2)	82(16)	770.7(2)	119(4)	1260.2(2)	58(4)
324.3(1)	325(4)	572.6(3)	25(6)	778.5(1)	830(7)	1274.7(6)	20(4)
336.6(1)	206(4)	576.5(3)	37(8)	797.6(2)	150(7)	1288.8(3)	36(4)
357.9(2)*	477(8)	583.0(2)*	185(25)	804.6(2)	82(7)		
359.2(1)*	–	583.7(2)*	106(20)	825.1(2)	132(5)		
366.3(2)	64(4)	598.1(1)	\equiv 1000	830.0(12)	20(7)		

total Q value obtained is consistent with that for the 6116 keV α -decay line of ^{162}Re . The prompt coincidences between the α particles and γ rays restrict the possible multipolarity assignment for the 66 keV transition to being either $E1$ or $M1$, as any higher multiplicities would have half-lives that are too long. Intensity balance arguments from data obtained in the second experiment lead to an $M1$ assignment for this transition. The group of counts below the 66 keV peak in the inset to Fig. 2(c) is not associated with the fine structure peak.

The second experiment investigated excited states in ^{158}Ta by γ -ray spectroscopy. Although the statistics were insufficient to identify γ -ray transitions feeding the (2^-) ground state, prompt and delayed γ rays populating the 9^+ state in ^{158}Ta were identified by demanding time coincidences with ions implanted into the DSSDs that were followed within 175 ms

by a 6048 keV α particle [18]. The proposed level scheme for transitions observed in ^{158}Ta that feed, depopulate, and bypass the 19^- isomer is shown in Fig. 3. The energies and relative intensities of ^{158}Ta γ rays measured promptly in the present experiment are presented in Table I, while the delayed transitions are presented in Table II.

Figure 4(a) shows the energy spectrum of γ rays measured in the clover Ge detector at the focal plane of RITU within 30 μs of the implantation into the DSSDs of a selected ^{158}Ta ion, while Fig. 5(a) shows the corresponding spectrum measured in the planar Ge detector. Figures 4(b) and 4(c) show the energy spectra of γ rays observed in coincidence with the 1002 keV and 746 keV transitions, respectively. Analysis of these γ -ray coincidences between the individual crystals of the clover Ge detector demonstrates that the 253 keV, 598 keV, and

TABLE II. Energies and relative intensities of γ -ray transitions observed at the focal plane in the present work. The intensities of the 66 keV and 160 keV transitions were measured using the planar Ge detector, while the remaining transitions were measured using the clover Ge detector. Intensities measured in the planar Ge detector have been normalised to those from the clover Ge detector by comparing the intensity of the 253 keV peak in both detectors. Intensities corrected for internal conversion are also given for these cases, assuming no multipole mixing and using conversion coefficients from Ref. [28]. The transition marked with an asterisk (*) is an unresolved multiplet.

E_γ (keV)	I_γ (Delayed)	Assigned ML	I_γ (Delayed, ICC corrected)	E_γ (keV)	I_γ (Delayed)	Assigned ML	I_γ (Delayed, ICC corrected)
66.1(2)	149(8)	$M1$	516(29)	599.2(8)	\equiv 1000	$E2$	\equiv 1000
159.5(2)	20(2)			634.5(8)	29(5)		
253.5(6)	911(47)	$E2$	1023(53)	708.1(9)	115(8)	$E3$	116(8)
273.7(6)*	40(6)			747.2(9)	488(26)	$E2$	486(26)
418.5(7)	48(6)	$M2$	60(8)	778.8(10)	579(31)	$E2$	576(31)
435.9(7)	58(7)			782.2(10)	50(7)		
439.2(8)	42(6)			1001.6(11)	984(51)	$E3$	980(51)
583.9(8)	75(7)	$M1$	77(7)				

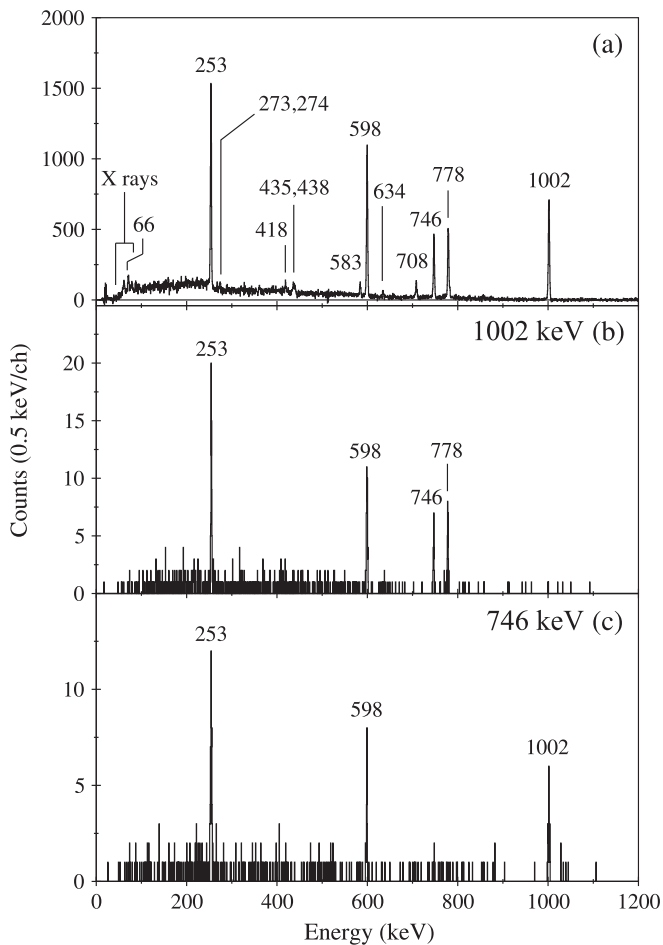


FIG. 4. (a) Energy spectrum of γ rays measured in the clover Ge detector within $30 \mu\text{s}$ of the implantation into the DSSDs of ions that were followed within 175 ms by a 6048 keV α decay characteristic of the 9^+ state in ^{158}Ta . Energy spectra of the γ rays in (a) that were measured in coincidence with (b) the 1002 keV transition and (c) the 746 keV transition. For the spectra in (b) and (c) the crystals of the clover Ge detector were treated as individual detectors.

1002 keV transitions are mutually coincident. The 746 keV and 778 keV transitions are also in coincidence with these γ rays, but they are not in coincidence with each other. However, 746 keV γ rays observed in the clover Ge detector were found to be in prompt coincidence with 66 keV γ rays observed in the planar Ge detector [see Fig. 5(b) and 5(c)].

The relative ordering of the 253 keV, 598 keV, and 746 keV/778 keV transitions was established through the prompt coincidences observed in JUROGAM, for example with the 474 keV and 438 keV transitions. The angular intensity ratios of the 253 keV, 598 keV, 746 keV, and 778 keV transitions measured using the JUROGAM array are consistent with those of known stretched $E2$ transitions measured during the same experiment. The 66 keV transition must be of $M1$ multipolarity if its intensity is to balance that of the 746 keV transition measured in the focal plane Ge detectors. An unobserved 34 keV $M1$ transition is proposed to account for the coincidences observed with 778 keV γ rays.

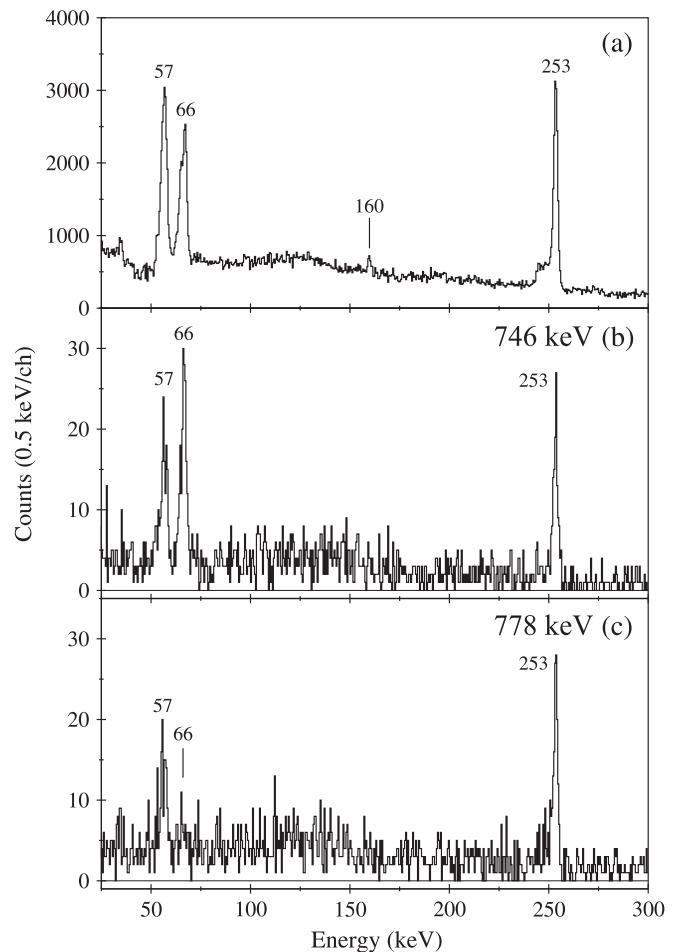


FIG. 5. (a) Energy spectrum of photons measured using the planar Ge detector occurring within $30 \mu\text{s}$ of ions implanted into the GREAT DSSDs that were followed within 175 ms by a 6048 keV α decay of ^{158}Ta . Energy spectra of photons from (a) observed in coincidence with (b) a 746 keV γ ray or (c) a 778 keV γ ray in the clover Ge detector. The ratio of x-ray intensities in (b) is inconsistent with that expected for tantalum, indicating a γ ray overlaps the K_{β} peak. The ratio in (c) is consistent with the literature value.

In addition to the γ rays discussed above, there are weaker peaks evident in Fig. 4(a) at energies of 273 keV, 418 keV, 435 keV, 438 keV, 583 keV, 634 keV, and 708 keV, while in Fig. 5(a) there is also peak at 160 keV. Of these γ -ray transitions, only the 418 keV and 708 keV lines are absent from the energy spectrum of prompt ^{158}Ta γ rays observed in JUROGAM that is shown in Fig. 6(a). On this basis we assign them as γ -ray transitions in parallel with the 1002 keV transition that directly depopulate the isomer. The 583 keV γ is assigned as a transition connecting the state populated by the 418 keV γ ray to the yrast 16^+ state. Lifetime and intensity balance considerations suggest $M2$ and $M1$ multiplicities for the 418 keV and 583 keV transitions, respectively. Lifetime arguments suggest that the 708 keV transition could be of $E3$ multipolarity. Analysis of the prompt γ -ray coincidence data suggests that the same state is populated by the 503 keV and 862 keV γ -ray transitions and has a decay path that proceeds via the 273 keV transition. A 74 keV transition is proposed

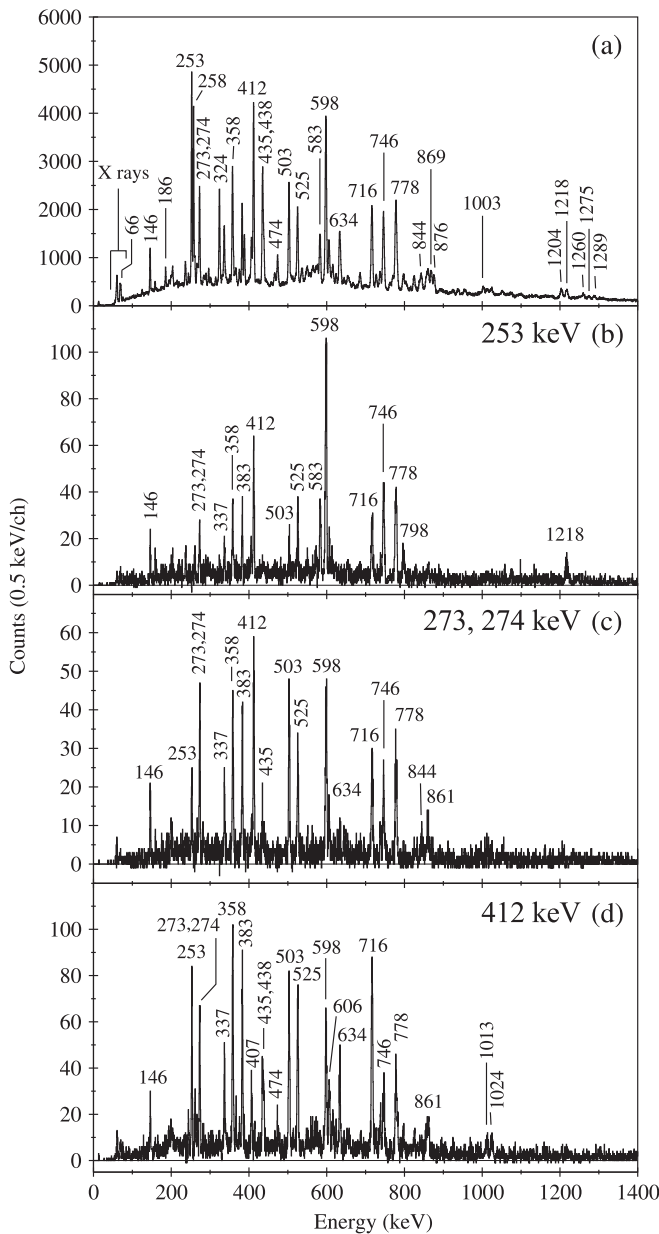


FIG. 6. (a) Energy spectrum of γ rays correlated with ^{158}Ta α tagged recoils with a recoil- α correlation time of 175 ms at the target position. Energy spectra of these γ rays measured in coincidence with (b) the 253 keV transition, (c) the 273 keV and 274 keV transitions, and (d) the 412 keV transition.

to explain coincidences observed between the transitions populating the 1957 keV state and those depopulating the state at 1885 keV.

Many other transitions that bypass the 19^- isomer and feed the low-lying states were observed in the prompt γ -ray data, as can be seen from the γ -ray coincidence energy spectra shown in Fig. 6(b)–6(d). Analysis of these and other coincidence spectra indicates that the level scheme is rather fragmented, but nevertheless extends up to an excitation energy of ~ 6.6 MeV above the 9^+ state. It was not possible to obtain definitive multipolarity assignments for many of the γ rays, so it is not

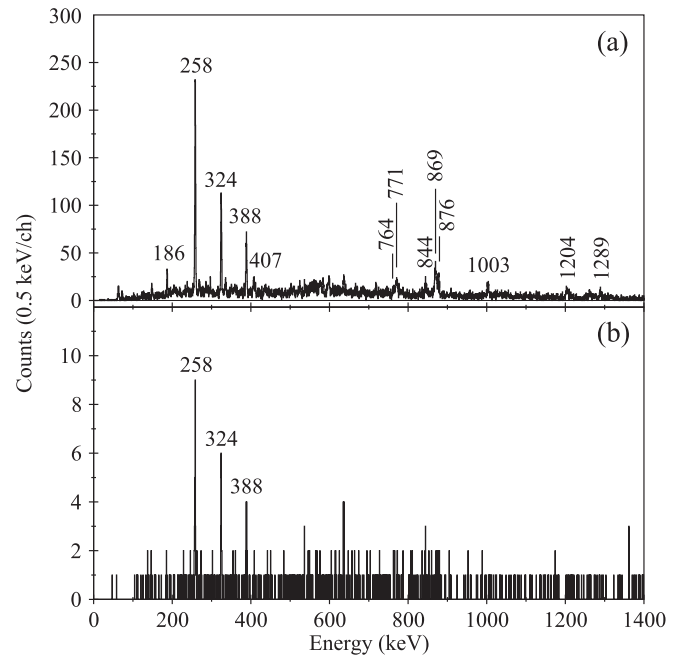


FIG. 7. (a) Energy spectrum of γ rays measured at the target position and correlated with recoils that were followed within 30 μs of implantation by a γ -ray transition observed in Fig. 4(a) and within 175 ms by a 6048 keV ^{158}Ta α decay. (b) Energy spectrum of γ rays measured at the target position correlated with recoils that were followed within 32 μs by an 8644 keV ^{158}Ta α decay.

clear what maximum spin values have been reached. Although comparison of the proposed level scheme with those of its isotones ^{152}Ho [29] and ^{154}Tm [30] suggests that states such as the 5273 keV level may correspond to specific configurations, given the uncertainties about their spin values, caution is required when speculating about their interpretation.

Prompt γ -ray transitions measured in JUROGAM that populate the 19^- isomer ($t_{1/2} = 6.1(1)\mu\text{s}$ [16]) were also identified. Figure 7(a) shows γ rays from Fig. 6(a) where the implanted ions were followed within 30 μs by a 253 keV, 598 keV, 708 keV, 746 keV, 778 keV, or 1002 keV γ ray depopulating the isomer. Figure 7(b) shows γ rays measured in delayed coincidence with ions that were followed within 32 μs by an 8644 keV α decay from the 19^- isomer. Although the latter spectrum has fewer counts, the strongest transitions from (a) are clearly present in (b) and provide additional evidence that the α particles and γ rays emanate from the same state in ^{158}Ta .

While most of the strongest transitions have been placed in the excitation level scheme, there are several weaker transitions that could not be placed unambiguously. For example, a 686 keV transition was observed in coincidence with 435 keV and 474 keV γ rays. One difficulty in this particular case was that the 435 keV transition is a self-coincident doublet. The 435 keV transition is also noteworthy in that it is coincident with a 782 keV transition, which appears to be distinct from the 778 keV transition that is coincident with, for example, the 598 keV transition. However, the 634 keV transition appears to be coincident with both the 778 keV and 782 keV transitions.

An unobserved 33 keV transition from the state at 1251 keV could connect the 634 keV transition with the 435 keV and 782 keV transitions.

The 273 keV transition is proposed to be an unresolved triplet, with two components populating and depopulating a state at 1684 keV. The third component is a decay path out of the state at 5273 keV into the 5002 keV state, eventually populating the 9^+ state rather than the 19^- isomer. The coincidences of the 146 keV and 383 keV transitions with 273 keV γ rays are stronger than those with 253 keV γ rays, whereas the converse is true for the 525 keV and 412 keV transitions. It should also be noted that 583 keV and 634 keV γ rays are coincident with prompt γ rays that populate the 9^+ state, while 584 keV and 637 keV γ rays feed the 19^- isomer. Although these γ rays are not mutually coincident, they do cause ambiguities. For example, an 805 keV transition observed in coincidence with 583 keV and 435 keV γ rays could not be placed in the level scheme. Finally, the 358 keV transition is coincident with 359 keV γ rays.

An energy level at 2737 keV was identified, but is not shown in Fig. 3 for clarity. This state decays by the emission of 1074 keV γ rays to the 16^+ state at 1663 keV and by 1053 keV γ -ray emission to the 1684 keV state. A 727 keV transition was observed to be in coincidence with 825 keV and 857 keV γ rays. All three γ rays were observed in coincidence with the 412 keV transition, but could not be placed with confidence in the level scheme. Placing all of the transitions discussed above into the level scheme and removing the ambiguities arising from unresolved multiplet transitions remain as challenges for future studies of ^{158}Ta .

IV. DISCUSSION

The lowest-lying states in ^{158}Ta are governed by the three valence neutrons outside the $N = 82$ core coupling with an odd proton. The proposed configurations of the (2^-) and 9^+ states are $\pi d_{3/2} \otimes \nu f_{7/2}$ and $\pi h_{11/2} \otimes \nu f_{7/2}$, respectively [18], while those of the sequence of yrast states from the 10^+ state to the 16^+ state are $\pi h_{11/2} \otimes \nu f_{7/2}^2 h_{9/2}$ [16]. This sequence fits very well into the systematics of excited states of $N = 85$ isotones that are plotted in Fig. 8. The reduced excitation energy difference between the 9^+ and 10^+ states in ^{158}Ta compared with lighter odd-odd isotones resembles the trend seen in the corresponding systematics for odd-A isotones. An explanation for this trend is that the attractive interaction between $\pi h_{11/2}$ protons and $\nu h_{9/2}$ neutrons increases as protons are added to the $\pi h_{11/2}$ orbital. Establishing this energy difference in ^{156}Lu to bridge the gap in the systematics between ^{154}Tm and ^{158}Ta is a challenge for future experiments.

In the isotones ^{152}Ho and ^{154}Tm states with spins and parities of 11^+ and 13^+ that are built upon the 9^+ isomer have been identified and interpreted as a $\pi h_{11/2}^3 \otimes \nu f_{7/2}^3$ configuration [29,30]. The state identified in the present work at 778 keV above the 9^+ isomer is a candidate for the corresponding 11^+ state in ^{158}Ta , but there is no obvious candidate for the 13^+ state. It is possible that this state lies close to or above the 14^+ state at 1411 keV and is weakly populated, but since the systematics of these odd-spin states

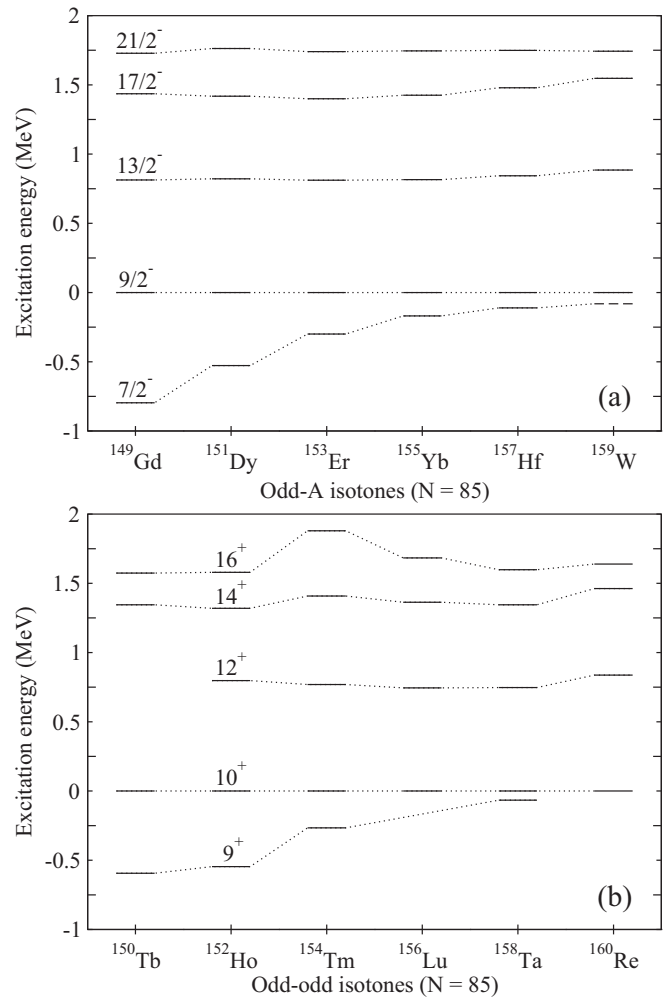


FIG. 8. Systematics of energy levels in $N = 85$ isotones relative to (a) the $9/2^-$ state in odd-A isotones, and (b) the 10^+ state in odd-odd isotones [10,29–36]. A clear decrease in the separation between the $9/2^-$ and $7/2^-$ states and the 10^+ and 9^+ states occurs as Z increases. The $7/2^-$ level in ^{159}W is shown by the dashed line at 81 keV, which should be regarded as a lower limit [10].

presently do not extend beyond ^{154}Tm , it is not possible to draw any definite conclusions.

One mechanism for generating states with spins greater than $16 \hbar$ is to excite one or more of the neutrons into a $\nu i_{13/2}$ orbital. The suggested structure of the 19^- isomer as a $\pi h_{11/2}^{-3} \otimes \nu f_{7/2} h_{9/2} i_{13/2}$ state, analogous to that of an isomer in ^{152}Ho [29], is an example of this. The full alignment of these six valence particles is expected to produce a state with spin and parity 28^- . In ^{152}Ho this state is isomeric with a 47 ns half-life and lies at 5838 keV, which is 2978 keV above the 19^- isomer [29], while in ^{154}Tm a state at 6141 keV was proposed as a candidate for this configuration [30]. The state established in the present work at 5273 keV could correspond to this configuration in ^{158}Ta , lying 2608 keV above the 19^- isomer. This state has a fragmented decay pattern and is fed by high-energy transitions, which could indicate pair-breaking excitations. Alternatively, it is possible that the 28^- state is also

isomeric in ^{158}Ta and consequently its decays may not have been observed in coincidence with the prompt γ rays at the target position.

An alternative mechanism for generating spins greater than $16\hbar$ is through the creation of higher-seniority states by breaking a pair of $\pi h_{11/2}$ protons and aligning their angular momenta, with the neutrons remaining in $\nu f_{7/2}$ or $\nu h_{9/2}$ orbitals. The full alignment of the six valence nucleons in this case would produce a state with spin and parity 25^+ . This underlying structure could account for many of the states whose depopulation paths bypass the 19^- isomer, including the strongly populated states that decay by the sequence of γ rays with energies of 383 keV, 525 keV, and 412 keV. One of the decay paths from the 5273 keV state proceeds via a 273 keV transition that feeds in above this sequence and could involve a neutron transition from a $\nu i_{13/2}$ orbital to a $\nu h_{9/2}$ orbital.

Since the 9^+ state in ^{158}Ta is known to be unbound to proton emission by 594(14) keV [18], it follows that all excited states are also unbound. In Ref. [16] the stability against proton emission of the 19^- isomer, for which $Q_p = 3261(14)$ keV, was considered. Some of the excited states presented in this work lie at even higher excitation energies and could potentially have proton emission branches. However, predicting the most likely candidates for this would require knowledge of the spins and parities of these states, as well as those in the proton-decay daughter ^{157}Hf that might be populated. Further work is required to obtain the firm spin and parity assignments that are needed to allow reliable predictions to be made. From the experimental point of view, it might be possible to identify instances of this by selecting γ rays measured in JUROGAM that are associated with α decays of

^{157}Hf identified in GREAT. If γ -ray transitions assigned to ^{158}Ta are observed it could indicate that one or more excited states have proton emission branches. This would be a similar situation to the discovery of proton emission from excited states in lighter nuclei, such as ^{56}Ni and $^{58,59}\text{Cu}$ [37–40]. Alternatively, it might be possible to detect such protons directly using an array of silicon detectors placed around the target position. While such experiments will undoubtedly be challenging, they could open up many more proton-emitting states for study in the future. This is important because the scope for discovering further cases of proton emission from low-lying states in this region appears to be rather limited [41].

ACKNOWLEDGMENTS

This work has been supported through the UK Science and Technology Facilities Council (S.T.F.C.); the Academy of Finland under the Finnish Centre of Excellence Programme 2006–2011 (Nuclear and Accelerator Based Physics Contract No. 213503) and the Finnish Centre of Excellence Programme 2012–2017; Swedish Research Council (Contract No. 2010-3694); EURONS (European Commission Contract No. RII3-CT-2004-506065); ENSAR (the European Union Seventh Framework Programme Integrating Activities, Transnational Access Project No. 262010); and the U.S. Department of Energy, Office of Nuclear Physics, under Contract No. DEAC02-06CH11357. The UK/France (STFC/IN2P3) Loan Pool and GAMMAPOOL network are acknowledged for the EUROGAM detectors of JUROGAM. T.G., P.T.G., and C.S. acknowledge the support of the Academy of Finland, Contracts No. 131665, No. 111965, and No. 209430, respectively.

-
- [1] M. Petri, E. S. Paul, B. Cederwall, I. G. Darby, M. R. Dimmock, S. Eeckhauudt, E. Ganioglu, T. Grahn, P. T. Greenlees, B. Hadinia *et al.*, *Phys. Rev. C* **76**, 054301 (2007).
- [2] P. T. Wady, J. F. Smith, E. S. Paul, B. Hadinia, C. J. Chiara, M. P. Carpenter, C. N. Davids, A. N. Deacon, S. J. Freeman, A. N. Grint *et al.*, *Phys. Rev. C* **85**, 034329 (2012).
- [3] Z. Liu, D. Seweryniak, P. J. Woods, C. N. Davids, M. P. Carpenter, T. Davinson, R. V. F. Janssens, R. D. Page, A. P. Robinson, J. Shergur *et al.*, *Phys. Lett. B* **702**, 24 (2011).
- [4] D. Seweryniak, C. N. Davids, W. B. Walters, P. J. Woods, I. Ahmad, H. Amro, D. J. Blumenthal, L. T. Brown, M. P. Carpenter, T. Davinson *et al.*, *Phys. Rev. C* **55**, R2137 (1997).
- [5] D. Seweryniak, P. J. Woods, J. J. Ressler, C. N. Davids, A. Heinz, A. A. Sonzogno, J. Uusitalo, W. B. Walters, J. A. Caggiano, M. P. Carpenter *et al.*, *Phys. Rev. Lett.* **86**, 1458 (2001).
- [6] D. Seweryniak, C. N. Davids, A. Robinson, P. J. Woods, B. Blank, M. P. Carpenter, T. Davinson, S. J. Freeman, N. Hammond, N. Hoteling *et al.*, *J. Phys. G: Nucl. Part. Phys.* **31**, S1503 (2005).
- [7] M. G. Procter, D. M. Cullen, M. J. Taylor, G. A. Alharshan, L. S. Ferreira, E. Maglione, K. Auranen, T. Grahn, P. T. Greenlees, U. Jakobsson *et al.*, *Phys. Lett. B* **725**, 79 (2013).
- [8] D. Seweryniak, J. Uusitalo, P. Bhattacharyya, M. P. Carpenter, J. A. Cizewski, K. Y. Ding, C. N. Davids, N. Fotiades, R. V. F. Janssens, T. Lauritsen *et al.*, *Phys. Rev. C* **71**, 054319 (2005).
- [9] I. G. Darby, R. D. Page, D. T. Joss, J. Simpson, L. Bianco, R. J. Cooper, S. Eeckhauudt, S. Ertürk, B. Gall, T. Grahn *et al.*, *Phys. Lett. B* **695**, 78 (2011).
- [10] P. J. Sappale, R. D. Page, D. T. Joss, L. Bianco, T. Grahn, J. Pakarinen, J. Thomson, J. Simpson, D. O'Donnell, S. Erturk *et al.*, *Phys. Rev. C* **84**, 054303 (2011).
- [11] K. Lagergren, D. T. Joss, R. Wyss, B. Cederwall, C. J. Barton, S. Eeckhauudt, T. Grahn, P. T. Greenlees, B. Hadinia, P. M. Jones *et al.*, *Phys. Rev. C* **74**, 024316 (2006).
- [12] T. Bäck, B. Cederwall, K. Lagergren, R. Wyss, A. Johnson, D. Karlgren, P. Greenlees, D. Jenkins, P. Jones, D. T. Joss *et al.*, *Eur. Phys. J. A* **16**, 489 (2003).
- [13] M. J. Taylor, D. M. Cullen, M. G. Procter, A. J. Smith, A. McFarlane, V. Twist, G. A. Alharshan, L. S. Ferreira, E. Maglione, K. Auranen *et al.*, *Phys. Rev. C* **91**, 044322 (2015).
- [14] D. T. Joss, I. G. Darby, R. D. Page, J. Uusitalo, S. Eeckhauudt, T. Grahn, P. T. Greenlees, P. M. Jones, R. Julin, S. Juutinen *et al.*, *Phys. Lett. B* **641**, 34 (2006).
- [15] M. Wang, G. Audi, A. H. Wapstra, F. G. Kondev, M. MacCormick, X. Xu, and B. Pfeiffer, *Chin. Phys. C* **36**, 1603 (2012).

- [16] R. J. Carroll, R. D. Page, D. T. Joss, J. Uusitalo, I. G. Darby, K. Andgren, B. Cederwall, S. Eeckhauudt, T. Grahn, C. Gray-Jones *et al.*, *Phys. Rev. Lett.* **112**, 092501 (2014).
- [17] R. J. Carroll, R. D. Page, D. T. Joss, J. Uusitalo, I. G. Darby, K. Andgren, B. Cederwall, S. Eeckhauudt, T. Grahn, C. Gray-Jones *et al.*, *Acta Phys. Pol. B* **46**, 695 (2015).
- [18] C. N. Davids, P. J. Woods, J. C. Batchelder, C. R. Bingham, D. J. Blumenthal, L. T. Brown, B. C. Busse, L. F. Conticchio, T. Davidson, S. J. Freeman *et al.*, *Phys. Rev. C* **55**, 2255 (1997).
- [19] M. Leino, J. Äystö, T. Enqvist, P. Heikken, A. Jokinen, M. Nurmia, A. O. W. H. Trzaska, J. Uusitalo, K. Eskola, P. Armbruster *et al.*, *Nucl. Instrum. Methods Phys. Res. B* **99**, 653 (1995).
- [20] R. D. Page, A. N. Andreyev, D. E. Appelbe, P. A. Butler, S. J. Freeman, P. T. Greenlees, R.-D. Herzberg, D. G. Jenkins, G. D. Jones, P. Jones *et al.*, *Nucl. Instrum. Methods Phys. Res. B* **204**, 634 (2003).
- [21] K.-H. Schmidt, R. S. Simon, J.-G. Keller, F. Hessberger, G. Münzenberg, B. Quint, H.-G. Clerc, W. Schwab, U. Gollerthan, and C.-C. Sahm, *Phys. Lett. B* **168**, 39 (1986).
- [22] E. S. Paul, P. J. Woods, T. Davinson, R. D. Page, P. J. Sellin, C. W. Beausang, R. M. Clark, R. A. Cunningham, S. A. Forbes, D. B. Fossan *et al.*, *Phys. Rev. C* **51**, 78 (1995).
- [23] I. H. Lazarus, D. E. Appelbe, P. A. Butler, P. J. Coleman-Smith, J. R. Cresswell, J. S. Freeman, R. D. Herzberg, I. Hibbert, D. T. Joss, S. C. Letts *et al.*, *IEEE Trans. Nucl. Sci.* **48**, 567 (2001).
- [24] P. Rakhila, *Nucl. Instrum. Methods Phys. Res. A* **595**, 637 (2008).
- [25] D. Radford, *Nucl. Instrum. Methods Phys. Res. A* **361**, 297 (1995).
- [26] S. Hofmann, G. Münzenberg, F. P. Hessberger, W. Reisdorf, P. Armbruster, and B. Thuma, *Z. Phys. A* **299**, 281 (1981).
- [27] R. D. Page, P. J. Woods, R. A. Cunningham, T. Davinson, N. J. Davis, A. N. James, K. Livingston, P. J. Sellin, and A. C. Shotton, *Phys. Rev. C* **53**, 660 (1996).
- [28] T. Kibédi, T. W. Burrows, M. B. Trzhaskovskaya, P. M. Davidson, and C. W. Nestor Jr., *Nucl. Instrum. Methods Phys. Res. A* **589**, 202 (2008).
- [29] S. André, C. Foin, D. Santos, D. Barnéoud, J. Genevey, C. Vieu, J. S. Dionisio, M. Pautrat, C. Schück, and Z. Meliani, *Nucl. Phys. A* **575**, 155 (1994).
- [30] C. Foin, A. Gizon, J. Genevey, J. Gizon, P. Paris, F. Farget, D. Santos, D. Barnéoud, and A. Plochocki, *Eur. Phys. J. A* **14**, 7 (2002).
- [31] M. Piiparinen, R. Pengo, Y. Nagai, E. Hammarén, P. Kleinheinz, N. Roy, L. Carlén, H. Ryde, T. Lindblad, A. Johnson *et al.*, *Z. Phys. A* **300**, 133 (1981).
- [32] G. Duchêne, C. M. Petrache, C. W. Beausang, F. A. Beck, T. Byrski, D. Curien, P. J. Dagnall, S. Flibotte, P. D. Forsyth, G. de France *et al.*, *Z. Phys. A* **350**, 39 (1994).
- [33] M. Piiparinen, S. Lunardi, P. Kleinheinz, H. Backe, and J. Blomqvist, *Z. Phys. A* **290**, 337 (1979).
- [34] C. Foin, S. André, and D. Barnéoud, *Z. Phys. A* **305**, 81 (1982).
- [35] K. Y. Ding, J. A. Cizewski, D. Seweryniak, H. Amro, M. P. Carpenter, C. N. Davids, N. Fotiades, R. V. F. Janssens, T. Lauritsen, C. J. Lister *et al.*, *Phys. Rev. C* **64**, 034315 (2001).
- [36] A. F. Saad, C. T. Zhang, R. Collatz, P. Kleinheinz, R. Menegazzo, R. Broda, K. H. Maier, H. Grawe, M. Schramm, R. Schubart *et al.*, *Z. Phys. A* **351**, 247 (1995).
- [37] D. Rudolph, C. Baktash, J. Dobaczewski, W. Nazarewicz, W. Satula, M. J. Brinkman, M. Devlin, H.-Q. Jin, D. R. LaFosse, L. L. Riedinger *et al.*, *Phys. Rev. Lett.* **80**, 3018 (1998).
- [38] D. Rudolph, C. Baktash, M. J. Brinkman, E. Caurier, D. J. Dean, M. Devlin, J. Dobaczewski, P.-H. Heenan, H.-Q. Jin, D. R. LaFosse *et al.*, *Phys. Rev. Lett.* **82**, 3763 (1999).
- [39] D. Rudolph, C. Andreoiu, C. Fahlander, R. J. Charity, M. Devlin, D. G. Sarantites, L. G. Sobotka, D. P. Balamuth, J. Eberth, A. Galindo-Uribarri *et al.*, *Phys. Rev. Lett.* **89**, 022501 (2002).
- [40] C. Andreoiu, T. Dossing, C. Fahlander, I. Ragnarsson, D. Rudolph, S. Åberg, R. A. E. Austin, M. P. Carpenter, R. M. Clark, R. V. F. Janssens *et al.*, *Phys. Rev. Lett.* **91**, 232502 (2003).
- [41] R. D. Page, *Phys. Rev. C* **83**, 014305 (2011).